Engineering and Technology Journal 40 (02) (2022) 422- 427

Engineering and Technology Journal
Journal homepage: https://etj.uotechnology.edu.iq

Physical Properties of Pure Gold Nanoparticles and Gold Doped ZnO Nanoparticles Using Laser Ablation in Liquid For Sensor Applications

Nabaa K. Hassan, Makram A. Fakhri *, Evan T. Salim

Laser and Optoelectronic Engineering Dept., University of Technology-Iraq, Alsina'a street, 10066 Baghdad, Iraq.
*Corresponding author Email: makram.a.fakhri@uotechnology.edu.iq

HIGHLIGHTS

- Using laser ablation of pure gold targets to obtain gold Nano rods.
- A cheap pulsed laser source was used to prepare gold Nano rods.
- Zinc-doped gold Nano rods were prepared to fabricate optical and biological sensors.
- The fabricated Zinc-doped gold Nano rods shave superior optical, structural, and morphological properties and can be used in different sensors.

ARTICLE INFO

Handling editor: Ivan A. Hashim

Keywords: Laser ablation in ethanol
Optical analysis; Gold Nano roads
Refractive Index Sensors

ABSTRACT

In this paper, the effect of using laser ablation of pure gold targets to obtain gold Nano rods and for pure zinc targets to obtain zinc oxide nanoparticles was studied separately in ethanol using an Nd:YAG laser tattoo removal (nanosecond pulses) and then mixing the resulting mixtures to obtain gold dopant with zinc oxide. Transmission electron microscopy (TEM), (XRD) X-Ray Diffraction and the optical properties were used to characterize the pure gold Nano rods, ZnO nanoparticles, and Au doped ZnO nanoparticles. Based on XRD and TEM, the results revealed the properties of the produced gold Nano roads. The obtained results indicated that the gold Nano rods produced by the 1064nm laser have superior optical, structural, and morphological properties and can be used in different sensors.

1. Introduction

Nano rods and Nanoparticles (Nps) of noble metals have recently emerged as intriguing materials due to their unique features and critical applications in various scientific fields [1, 2]. The production of metallic Nano rods, mostly silver or gold, has sparked interest due to their (SPR) surface Plasmon resonance-related features, which could be helpful in biological applications [3, 4]. The control of physical parameters of the ablated Nano rods, like the surface functionalization, shape, and size, is the most essential concern in Au NP production [5, 6]. Pure and Doped Gold Nano rods focus on the Nano bio, Nano-Photonics, and Nano medicine applications due to their chemical stability and prominent optical features [7, 8].

As structure versatile surface-upgraded Raman dissipating based labels for illness focusing on and conclusion, Gold Nano rods can also make a difference in malignant growth imaging by photoacoustic or light dispersing. Biotechnology, material sciences, PC sciences, prescriptions, pharmacy stores, and design use nanotechnology to stress materials on 10-9 meter scales. In the ninth century, Mesopotamian individuals first used nanotechnology to create a glossy effect in pottery [9, 10].

Michael Faraday discovered ruby gold nanoparticles (Au NPs) for the first time in 1857, laying the groundwork for advanced nanotechnology [11, 12]. The flounce of used laser, spot estimation, pulse width, repetition rate, and wavelength can all constrain the structural and morphological characteristics of the generated NPs [13, 14].

The tattoo removal laser of a powerful target submerged in a fluid environment has become an increasingly necessary "top-down" method for producing nanostructured materials [15, 16]. The elimination of a strong target placed in a fluid medium produces NP and Nano rods in this technique. Controlling the size, focus, chemical composition, and practical features of the Nano rods are possible by altering the laser settings and the concept of the surrounding fluid media. For this reason, a variety of types of the used lasers have been suggested, including femtosecond, picosecond, and nanosecond lasers with different wavelengths ranging from the ultraviolet (0.248 µm) to infrared (1.064 µm) [17, 18]. In the last few years, another method for

http://doi.org/10.30684/etj.v40i2.2242
Received 20 June 2021; Accepted 17 August 2021; Available online 25 February 2022
2412-0758/University of Technology-Iraq, Baghdad, Iraq

amalgamating gold nanoparticles that rely on laser removal of the mass metal in the fluid has emerged [5, 19, and 20]. Mafune' et al. have shown that using the second harmonic of an Nd:YAG laser (0.532 nm) and a surfactant such as sodium dodecyl sulfate (SDS), it is also possible to achieve excellent control over the elements of nanoparticles [21]. Cheng et al. [22] studied the photocatalytic properties of the hybrid TiO-ZnO nanostructures prepared using the site-specific deposition method of the amorphous titanium dioxides on the tips of zinc oxide Nano rods. Comparing the pure oxides (ZnO TiO_2) nanoparticles with the hybrid TiO_2-ZnO nanostructures, the hybrid nanostructures present a higher catalytic activity due to the improved charge transfer and separation process caused by the novel Nano hetero structures with the micro interfaces. Misra et al. [23] synthesized the core-shell (Au@ZnO) nanoparticle with flower-like structures. The core values of the Au have increased with the activity of the ZnO photo catalytic as a result of the enhanced absorption of the light and separation of the charges. Combining a noble metal with a single paired semiconductor using an easy and cheap processing method would be a great leap in favor of developing a new type of optical and biological sensor. Where in this manuscript, Au-doped zinc oxide Nanocrystals were fabricated by pulsed laser ablation method using the main mode length of the laser used for tattoo removal, which is a rather cheap device compared to the previously used lasers.

2. Experimental work

To extract a pure gold Nano rod, a 2.5 cm diameter circular High purity gold alloy was submerged in 5 ml (also same partitions for the Zn Target) of high purity ethanol and shook using the ultrasonic cleaner in the first stage. With continued shaking, we irradiate the gold metal using a pulsed Q-switched Nd-YAG tattoo removal laser at 1064 nm, applying energy of 2000 mJ/pulse and 200 pulses with a 12 cm lens (spot size: 0.8 mm2) to generate the Nano rods as shown in Figure 1, After a few seconds, it usually results in a red or purple coloring of the solution, and this is due to the formation of gold Nano rods. The same steps were applied for the Zn Target separately (After a few seconds, the solution's gray coloration usually results from the formation of zinc oxide Nanocrystals). The generated pure gold Nano road and gold doped ZnO Nanoparticles were tested using a UV-via double-beam spectrometer after the production process, X-ray diffraction investigation with a diffract meter system (x' pert pro-MRD PW3040) determined the phase structure of the nanoparticles and TEM.

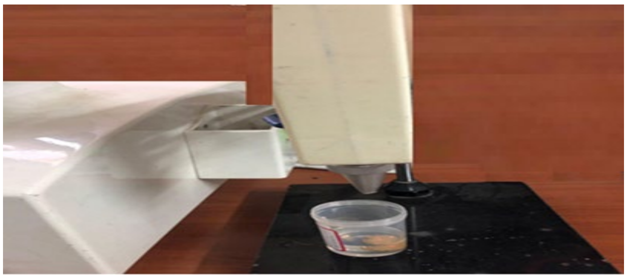

Figure 1: Laser ablation in solution was used to prepare gold colloid samples in an experimental setup

3. Results and Discussion

Figure 2 shows the XRD pattern for the produced: gold Nano rods, zinc oxides nanoparticles, and Golden doped ZnO NPs, respectively, by using the Pulsed Laser Ablation in Ethanol process with a Pulsed Laser of 1064 nm with 200 pulses. Figure 2 (a) displays the XRD of 1064 nm, with two distinct peaks at 2=38.13 and 44.22. Each of both peaks corresponded to the (fcc) lattice's standard Bragg reflections (111) and (200). Figure 2 (b) displays the XRD of 1064 nm, with five distinct peaks at 2=32.53, 34, 83, 35.94, 47.73, and 52.32. Each of the five peaks corresponded to the (fcc) lattice's standard Bragg reflections (100), (002), (101), (102), and (110), respectively. And finally, Figure (2 c) displays the XRD of 1064 nm, with seven distinct peaks at 2=32.53, 34, 83, 35.94, 38.13, 44.22, 47.73, and 52.32. Each of the seven peaks corresponded to the (fcc) lattice's standard Bragg reflections (100), (002), (101), (111), (200), (102), and (110), respectively. Therefore, it's clear that the presented peaks represent the gold Nano rods and ZnO NPs, in the same distinct peaks and exact values of Bragg reflections. Still, different intensities indicate a precise formation of the so-called nanoparticles (core-shell nanoparticles). This is entirely consistent with optical calculations and transmission electron microscopy, Which will be presented and discussed later in the next sections. These results exactly match the XRD, presented with previous results of [24-26].

To confirm the attachment between the gold nanowires and ZnO nanoparticles on the colloidal, the transmission electron microscopy (TEM) test was used. The observed results are shown in Figure 3(a, b, and c) below. Figure 3(a) presents the TEM result of the gold nanowires, also, Figure 3(b) presents the TEM result of the ZnO nanoparticles. Finally, Figure 3(c) shows the TEM result of the gold nanowires doped with ZnO nanoparticles. The aggregation of gold nanoparticles associated with ZnO has a profound effect on the absorption properties of these systems. The increase in the concentration of gold ions leads to an increase in the number of nanoparticles per ZnO molecule. Thus, there is a decrease in the distance between the nanoparticles. The TEM analysis shows that the gold particles in the zinc oxide solution are well dispersed with the spherical formation where it was clear that the gold core was playing an essential role in stabilizing the growth of nanoparticles in the presence of doping. This highlights the study of particles with or without golden nuclei. This stability can be explained by presenting the role of the gold core as a nanoparticle to form the zinc-based envelope. Distinctive images where gold particles appeared as small, dark, spherical shapes. In TEM images, the particles tend to agglomerate at the wavelength of 1064 nm, as they tend to clump and form larger sizes. It led to the formation of well-separated partials and increased the consistency of ZnO particles; these results exactly match the XRD presented results with previous results of [27-29].

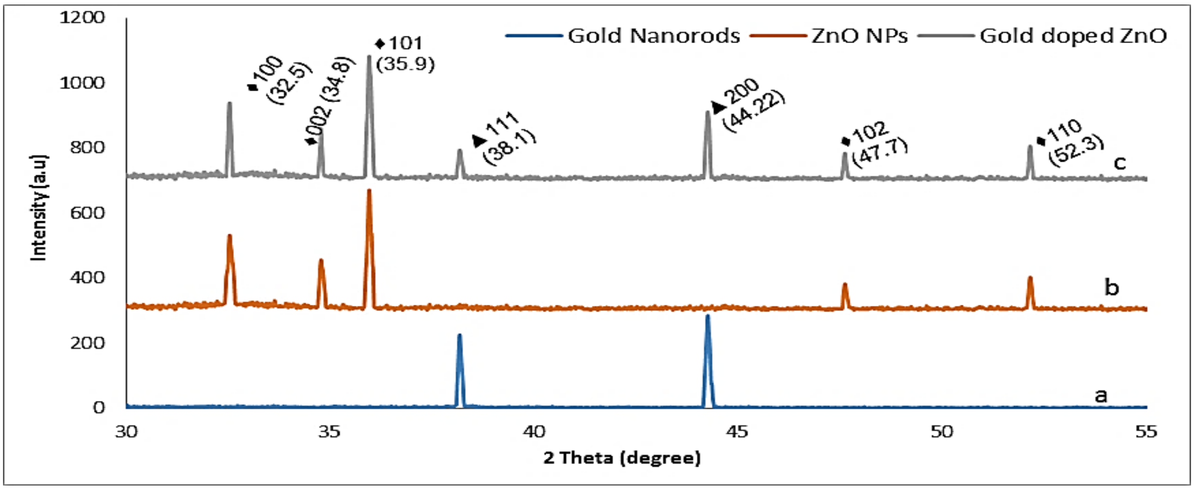

Figure 2: XRD analysis of gold nanoparticles and Gold doped ZnO nanoparticles

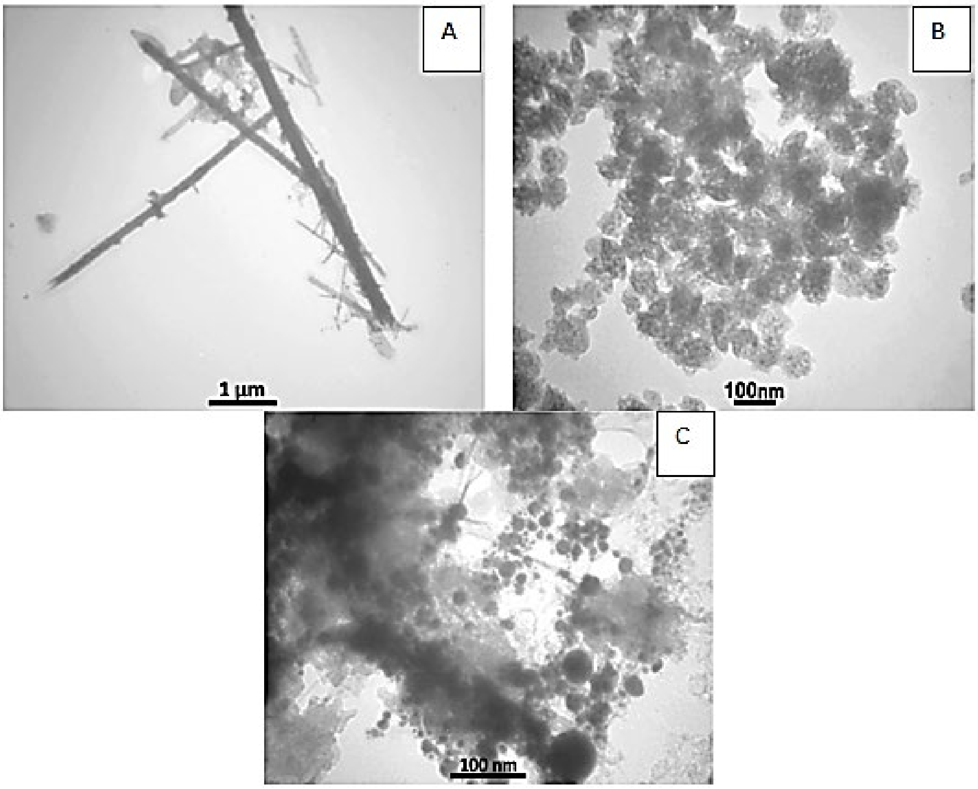

Figure 3: TEM results of (a) gold Nano rods (b) ZnO Nanoparticles, (c) gold doped ZnO nanoparticles

Figure 4 presents the transmission spectra of the gold Nano rods, ZnO NPs, and Au doped ZnO, respectively, in the colloidal suspension. The transmission values of the ablated Gold Nano rods, ZnO NPs, and Gold doped ZnO are almost identical at the start tests because we used the same tube (quartz tube) in the test. All tests give a high transmission value about 89% to 95%, but different in the transition response, where the Gold Nano rods start to work at the process region at 471 nm. It is evident at the presented curves; also the ZnO NPs begin to work at 231 nm, and it's clear that the gold doped ZnO has three regions, the first one at 220 nm for ZnO NPs, the second one at 320 nm for core-shell nanoparticles of gold as core and ZnO as shell and the third one at 466 nm for gold Nano rods. These results exactly match the XRD and TEM presented results and previous results of Long et al. [30-32].

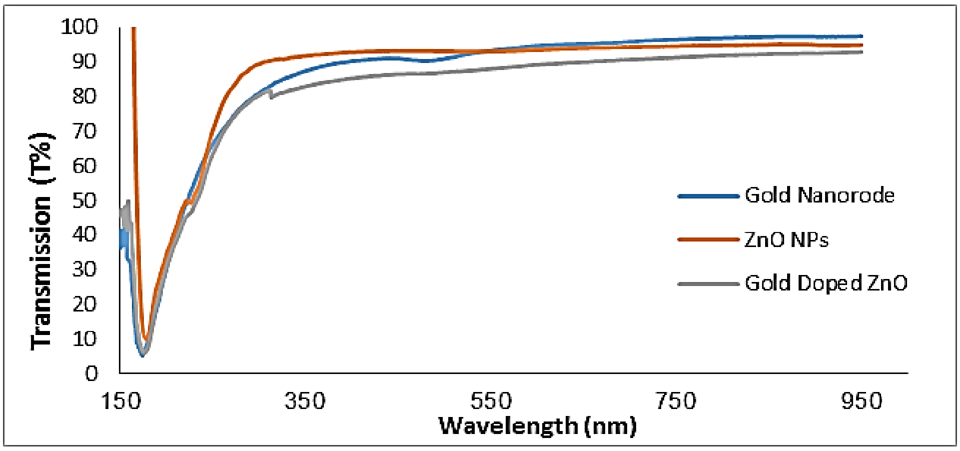

Figure 4: Transitions results of (a) gold Nano rods (b) ZnO Nanoparticles, (c) gold doped ZnO nanoparticles

Figure 5 shows the spectra of the relation between the photon energy and $(\alpha h\upsilon)^2$ for the gold Nano rods, ZnO NPs, and Au doped ZnO respectively in the colloidal suspension to estimate the values of the optical energy bandgap for all different colloidal suspensions ablated using PLA in ethanol. All presented results give a varying value of optical band gapes related to other Nano rods and nanoparticles and doped (core-shell). The Gold Nano rods present a bandgap value of 5.1 eV related to the gold Nano rods work region at 471 nm. It is clear at the presented curves. Also, the ZnO NPs present a bandgap value of 2.38 eV related to the ZnO NPs work region at 231 nm. Finally, the gold doped ZnO gives two regions: the first one at 3.3 eV related to 320 nm for core-shell nanoparticles of gold as core and ZnO as shell, and the second one at 4.2 eV that related to 466 nm for gold Nano rods. These results exactly match the XRD and TEM presented results, these results exactly match the XRD, and TEM presented results and with previous results of Refs. [33-35].

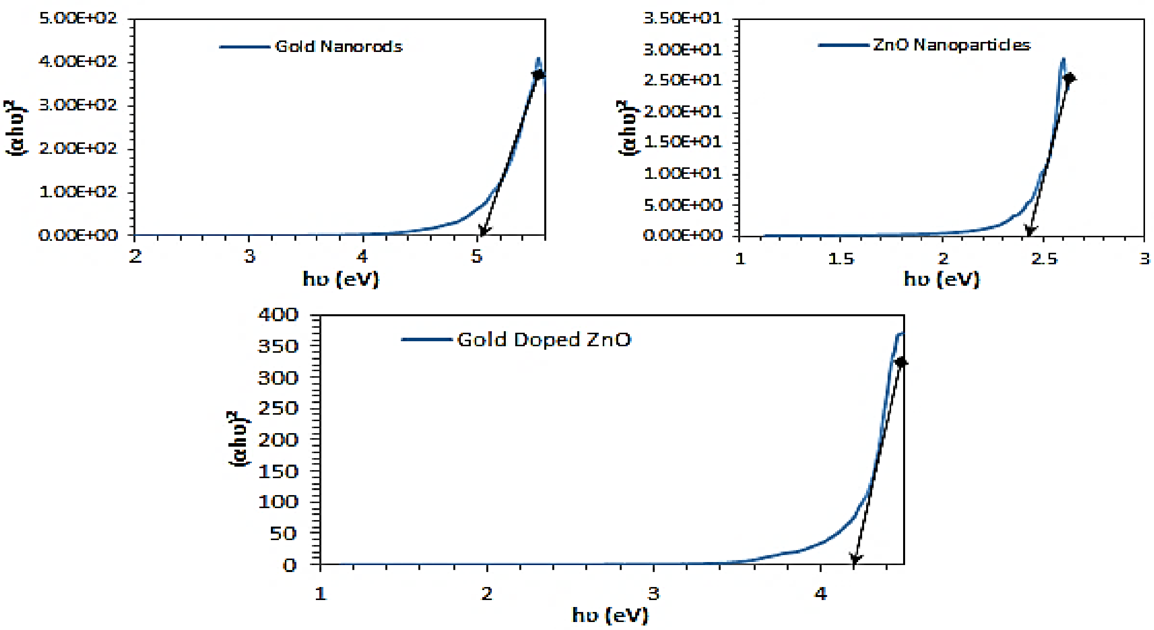

Figure 5: Optical band gap results of (a) gold Nano rods (b) ZnO Nanoparticles, (c) gold doped ZnO nanoparticles

4. Conclusions

A nanosecond tattoo removal Q-switched Nd:YAG pulsed laser at 1064 nm was used to ablated gold Nano rods, ZnO NPs, and Gold doped ZnO NPs in ethanol using the PLA method. The Structural (XRD), morphological (TEM), and Optical (T%, and E.g.) properties for the colloidal suspension were estimated and tested. The XRD results present the synthetic results showed the appearance of two dominant peaks representing gold Nano rods in the gold assays, and five peaks representing zinc oxide nanoparticles, including two prevalent peaks. The TEM results show from the TEM analysis that the gold particles in the zinc oxide solution are well dispersed with the spherical formation. Furthermore, it was clear that the gold core played an important role in stabilizing the growth of nanoparticles in the presence of doping and all particles' diameters less than 50 nm. Finally, the optical results show a high transmission and energy gap of 3.3 eV related to 320 nm for core-shell nanoparticles of gold as core and ZnO as shell, and the second one is at 4.2 eV that related to 466 nm for gold Nano rods.

Author contribution

All authors contributed equally to this work.

Funding

This research received no specific grant from any funding agency in the public, commercial, or not-for-profit sectors.

Data availability statement

The data that support the findings of this study are available on request from the corresponding author.

Conflicts of interest

The authors declare that there is no conflict of interest.

References

[1] E. Solati, D. Dorranian, Comparison between silver and gold nanoparticles prepared by pulsed laser ablation in distilled water, J. Clust. Sci., 26 (2015) 727-742. http://dx.doi.org/10.1007/10876-014-0732-2

[2] H. S. Ali, M. A. Fakhri, Z. Khalifa, Optical and structural properties of the gold nanoparticles ablated by laser ablation in ethanol for biosensors , J. Phys. Conf. Ser., 1795 (2021) 012065. https://doi.org/10.1088/1742-6596/1795/1/012065

[3] D. Riabinina, J. Zhang, M. Chaker, D. Ma, Size control of gold nanoparticles synthesized by laser ablation in liquid Media, ISRN Nanotechnology, 2012 (2012) 1-5. http//doi.org/10.5402/2012/297863

[4] K. I. Hassoon, S. H. Sabeeh, M. A. Khalaf, ZnO nano particles (NPs) properties prepared by liquid phase laser ablation (LPLA), Al-Nahrain , J. Sci., 20 (2017) 70-77. http://dx.doi.org/10.22401/JNUS.20.1.10

[5] V. Amendola, S. Polizzi, M. Meneghetti, Laser ablation synthesis of gold nanoparticles in organic solvents, Phys. Chem. B, 110 (2006) 7232-7237. http://dx.doi.org/10.1021/jp0605092

[6] Z.Yan, D. B.Chrisey, Pulsed laser ablation in liquid for micro-/nanostructure generation, Jo. Photo. a Photo. C: Photo. Reviews, 13 (2012) 204-223. https://doi.org/10.1016/j.jphotochemrev.2012.04.004

[7] F. Correard, K. Maximova, M. Estève, C. Villard, M. Roy, A. Al-Kattan, M. Sentis, M. Gingras, A. V Kabashin, D. Braguer, Gold nanoparticles prepared by laser ablation in aqueous biocompatible solutions : assessment of safety and biological identity for Nano medicine applications, Int. J. Nanomedicine., 9 (2014) 5415–5430. https://doi.org/10.2147/IJN.S65817

[8] A. Salah Aldeen, Z. H. Tawfiq, M. A. Fakhri, Gold nanoparticles in liquid based on photonic crystal fiber PCF for sensors application, Defect. Diffus. Forum, 398 (2020) 23-28. https://doi.org/10.4028/www.scientific.net/DDF.398.23

[9] S. M. Faydh, A. K. Al-Ogaili, E. T. Salim, Effect of the laser shock processing on wear resistance of brass alloy, Eng. Tech. J., 32 (2014) 998-1008. https://dx.doi.org/10.30684/ETJ.32.5B.16

[10] Z. H. Tawfiq, S. A. Adnan, M. A. Fakhri, R. K. Hamad, Structural, morphological and optical properties of gold nanoparticles using laser ablation in liquid for sensor applications, Iraqi J. Comp. Commun. Comt. Sys. Eng., 19 (2019) 30-35. https://doi.org/10.33103/uot.ijccce.19.4.4

[11] M. Das, K. H. Shim, S. S. A. An, D. K.Yi, Review on gold nanoparticles and their applications, Toxicol. Environ. Health. Sci., 3 (2011) 193–205. https://doi.org/10.1007/s13530-011-0109-y

[12] D. Zhang, B. Gökce, S. Barcikowski, Laser synthesis and processing of colloids: fundamentals and applications, Chem. Rev., 117 (2017) 3990–4103. https://dx.doi.org/10.1021/acs.chemrev.6b00468

[13] N. Mirghassemzadeh, M. Ghamkhari, D. Dorranian, Dependence of laser ablation produced gold nanoparticles characteristics on the fluence of laser pulse, Soft. Nano. sci. Let., 4 (2013) 101-106. https://dx.doi.org/10.4236/snl.2013.34018

[14] M.A. Fakhri, E. T. Salim, M. H. A. Wahid, A. W. Abdulwahhab, Z. T. Salim, U. Hashim, Heat treatment assistedspin coating for LiNbO3 films preparation: their physical properties, J. Phys. Chem. Solids., 131 (2019) 180-188. https://doi.org/10.1016/j.jpcs.2019.03.033

[15] J. Sylvestre, S. Poulin, A. V. Kabashin, E. Sacher , M. Meunier, J. H. T. Luong, Surface chemistry of gold nanoparticles produced by laser ablation in aqueous media, J. Phys. Chem. B, 108 (2004) 16864-16869. https://dx.doi.org/10.1021/jp047134+

[16] E. T. Salim, J. A. Saimon, M. K. Abood, M. A. Fakhri, Effect of ammonium concentration on structural, optical and morphological properties of H-Nb2O5 thin films—A novel study, Mat. Res. Express., 6 (2019) 046420. https://dx.doi.org/10.1088/2053-1591/aafc7a

[17] D. Riabinina , M. Chaker, Dependence of gold nanoparticle production on pulse duration by laser ablation in liquid media, Nanotechnology, 23 (2012) 135603. https://dx.doi.org/10.1088/0957-4484/23/13/135603

[18] V. Lehmann , U. Gösele, Porous silicon formation : A quantum wire effect, Appl. Phys. Let., 58 (1991) 856-858. https://doi.org/10.1063/1.104512

[19] M. P. Stewart , J. M. Buriak, Chemical and biological applications of porous silicon technology, Adv. Mater., 12 (2000) 859-869. https://dx.doi.org/10.1002/1521-4095(200006)12:12<859::AID-ADMA859>3.0.CO;2-0

[20] Z. H. Tawfiq, M. A. Fakhri, S. A. Adnan, Photonic crystal fibres PCF for different sensors in review, IOP. Conf. Series. Mater. Sci. Eng., 454 (2018) 012173. https://dx.doi.org/10.1088/1757-899X/454/1/012173

[21] C. Wang, X. Wang, B. Q. Xua, J. Zhao, B. Mai, P. Peng, G. Sheng, J. Fu, Enhanced photocatalytic performance of nanosized coupled ZnO/SnO2 photocatalysts for methyl orange degradation, J. Photochem. Photobiol. A., 168 (2004) 47-52. https://doi.org/10.1016/j.jphotochem.2004.05.014

[22] C. Cheng, A. Amini, C. Zhu, Z. Xu, H. Song, N. Wang, Enhanced photocatalytic performance of TiO2-ZnO hybrid nanostructures, Sci. Rep., 4 (2014) 4181. https://dx.doi.org/10.1038/srep04181

[23] M. Misra, P. Kapur, M. L. Singla, Surface plasmon quenched of near band edge emission and enhanced visible photocatalytic activity of Au@ZnO core-shell nanostructure, Appl. Catal. B: Environ., 150-151 (2014) 605-611. https://doi.org/10.1016/j.apcatb.2014.01.006

[24] Y. Xu, B. Yao, Y. F.Li, Z. H. Ding, J. C. Li, H. Z. Wang, D. Z. Shen, Chemical states of gold doped in ZnO films and its effect on electrical and optical properties, J. Alloys. Compd., 585 (2014) 479–484. https://doi.org/10.1016/j.jallcom.2013.09.199

[25] H. Xie, F. Ding, H. Mu, Effects of Au nanoparticles and ZnO morphology on the photocatalytic performance of Au doped ZnO/TiO2 films, Nanotechnol., 30 (2018) 085708. https://dx.doi.org/10.1088/1361-6528/aaf197

[26] M. A. Fakhry, F. A. Hattab, E. K. Hamed, Laser energy effects on optical properties of titanium di-oxide prepared by reactive pulsed laser deposition, Eng. Technol. J., 30 (2012) 3104-3111. https://dx.doi.org/10.30684/ETJ.30.17.12

[27] C. Byram, V. R. Soma, 2, 4-Dinitrotoluene detected using portable raman spectrometer and femtosecond laser fabricated Au–Ag nanoparticles and nanostructures, Nano-Structures . Nano-Objects, 12 (2017) 121–129. https://doi.org/10.1016/j.nanoso.2017.09.019

[28] M. Khenfouch, O. Bajjou, M. Baïtoul, N. Mongwaketsi, M. Maaza, J. W. Venturini, Optical properties and dynamics excitation relaxation in reduced graphene oxide functionalized with nanostructured porphyries, Opt. Mater., 42 (2015) 479–483. https://doi.org/10.1016/j.optmat.2015.02.006

[29] E. T. Salem , F. A. Mohamed , Preparation and characterization of MOS device using MgO Film as a dielectric material, Eng. Technol. J., 28 (2010) 6253-6262. https://dx.doi.org/10.30684/ETJ.28.21.4

[30] P. A. Prashanth , P. Singh, B. M. Nagabhushana, C. Shivakumara, G. M. Krishnaiah, H. G. Nagendra , H. M. Sathyananda , V. Chaturvedi, Effect of doping (with cobalt or nickel) and UV exposure on the antibacterial, anticancer, and ROS generation activities of zinc oxide nanoparticles, J. Asian. Ceram. Soc., 8 (2020) 1175-1187. https://dx.doi.org/10.1080/21870764.2020.1824328

[31] V. Perumal, U. Hashim, S. C. B. Gopinath, H. R. Prasad, L. Wei-Wen, S. R. Balakrishnan, T. Vijayakumar, R. A. Rahim, Characterization of gold-sputtered zinc oxide nanorods—a potential hybrid material, Nanoscale. Res. Lett., 11 (2016) 1-11. https://doi.org/10.1186/s11671-016-1245-8

[32] M. A. Fakhri, Effect of substrate temperature on optical and structural properties of indium oxide thin films prepared by reactive PLD method, Eng. Technol. J., 32 (2014) 1323-1330. https://dx.doi.org/10.30684/ETJ.32.5A.19

[33] C. Wang , T. Wang, Synthesis and optical properties of colloidal gold nanoparticles synthesis and optical properties of colloidal gold nanoparticles, J. Phys. Conf. Ser., 187 (2009) 012026. https://dx.doi.org/10.1088/1742-6596/187/1/012026

[34] S. B. Kolavekara, N.H. Ayachitb, G. Jagannathc, K. N.Krishnakanthd, S. V. Rao, Optical, structural and Near-IR NLO properties of gold nanoparticles doped sodium zinc borate glasses, Opt. Mater., 83 (2018) 34–42. https://doi.org/10.1016/j.optmat.2018.05.083

[35] E. T. Salim, H. H. Rashed, Laser pulses effect on the structural and optical properties of ZnO Nano particles prepared by laser ablation in water, Eng. Technol. J., 32 (2014) 198-207. https://dx.doi.org/10.30684/ETJ.32.2B.2